How do ~2° slopes fail in areas of slow sedimentation? A sensitivity study on the influence of accumulation rate and permeability on submarine slope stability

Morelia Urlaub[1], Antonis Zervos[2], Peter J. Talling[1], Doug G. Masson[1] and Chris I. Clayton[2]

1. National Oceanography Centre, European Way, Southampton SO14 3ZH, United Kingdom

2. School of Civil Engineering and the Environment, University of Southampton, Highfield, Southampton SO17 1BJ, United Kingdom

Abstract

Overpressure generation due to rapid sediment deposition can result in low effective stresses within the sediment column. It has been proposed that these large overpressures are the main preconditioning factor for causing large-scale submarine slope failure on passive continental margins, such as those in the Gulf of Mexico and offshore Norway. The rate of overpressure generation depends on the sedimentation rate, sediment compressibility and permeability. The Gulf of Mexico and the Norwegian continental slope have experienced comparatively high sediment input, but large-scale slope failure also occurs in locations with very low sedimentation rates such as the Northwest African continental margin. Here we show results from 2D numerical modelling of a 2° continental slope subjected to deposition rates of 0.15 m/ka. These results do not indicate any evidence for significant overpressure or slope instability. We conclude that factors other than overpressure must be fundamental for initiating slope failure, at least in locations with low sedimentation rates.

Keywords: Overpressure, continental margin, submarine landslide, slope stability modelling

1. Introduction

Submarine landslides that occur on the open slopes of passive continental margins represent the largest submarine mass flows on our planet. Perhaps the most remarkable feature of huge continental slope failures is that they occur in locations worldwide on gradients of just ~2°. Such low gradient slopes are almost always stable on land. We are yet to monitor one of these huge underwater landslides in action, and the reason(s) for such large-scale failure on such low gradients are contentious.

IODP Leg 308 drilling in the Gulf of Mexico recently confirmed that high excess pore pressures can be generated in areas of rapid sediment accumulation (Flemings et al. 2008). Low permeability prevents sufficiently rapid dewatering and excess pore pressures are produced that are up to 70% of the lithostatic weight. Numerical models using these IODP results suggest that a combination of rapid (up to 30 m/ka) sediment deposition caused by Mississippi River discharge and lateral fluid flow can generate slope failures (Flemings et al. 2008, Stigall and Dugan 2010). Similarly high sedimentation rates are likely to occur offshore from many major rivers and thereby cause large-scale slope failures. Sediment deposition at the margins of ice streams can also be very rapid and lead to excess pore pressures. Sedimentation rates of up to 36 m/ka occurred near the Storegga Slide headwall at the end of the last glaciation (Leynaud et al. 2007), although eventual failure of the Storegga Slide occurred ~7 ka after this peak sedimentation.

It might therefore be proposed that rapid sediment accumulation generating high excess pore fluid pressures are a major reason for large-scale continental slope failure on low (~2°) gradients. However, large-scale slope failures also occur on continental margins with much slower sediment accumulation rates, such as off the coast of Northwest Africa south of 26° N (Wynn et al. 2000). Deposition rates in this area do not exceed 0.15 m/ka, measured over the last 3.6 Ma (Ruddiman et al. 1988). Landslides in this area have a similar bedding-parallel slab-like morphology to failures like those in the Gulf of Mexico and the Storegga Slide (Haflidason et al. 2005, Twichell et al. 2009, Krastel et al., this volume), suggesting a common failure mechanism. Failure of the NW African slope has been attributed to overpressure (e.g. Antobreh and Krastel 2007) but a detailed analysis of how such overpressure might build up was not undertaken. Some key information and relationships of the three considered continental margins is given in Figure 1.

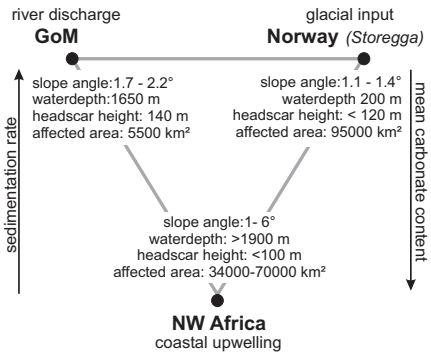

Fig. 1. Characteristics of continental margins and slides (mean values) discussed here (GoM = Gulf of Mexico).

1.1 Aims

Here we undertake a sensitivity analysis of how sediment accumulation rate and permeability influence the stability of low-angle continental slopes, starting with a one-dimensional column followed by a two-dimensional slope profile. The models are meant to be generic and broadly representative of a NW African type of continental margin. The model is not intending to mimic all the detailed aspects of this location. Our aims are to identify the situations in which particularly high excess pore fluid pressures might be generated, and whether slow sedimentation rates can produce high excess pore pressures that bring a slope close to failure, for reasonable values of sediment permeability. If we are unable to initiate slope failure through build up of high excess pore fluid pressures in this way, then slope failure in low sedimentation rate settings is more likely due to other factors such as internal sediment structures.

1.2 Proto-type Field Location – NW African Margin south of 26°N

The NW African continental margin is relatively uniform over long distances and is disrupted only by widely-spaced canyons. Pelagic and hemipelagic background sedimentation is dominant and originates from a continuous upwelling cell that produces large quantities of biologic material and is located at the upper slope (Sarnthein et al. 1982). Sediment cores recover fine-grained carbonate rich marls and oozes consisting mainly of planktonic shell fragments and terrigenous dust (e.g. Henrich et al. 2008). Sediment accumulation decreases offshore, with rates of up to 0.15 m/ka at the upper slope, and 0.01 m/ka at the mid and lower slope (Ruddiman et al. 1988, Henrich et al. 2008).

2. Methodology

2.1 Gibson's (1958) Approach to One-Dimensional Consolidation

Gibson's (1958) theory of 1D consolidation under constant deposition is a simple approach to estimate overpressure within a continuously growing clay layer. Key variables are sedimentation rate, time, Darcy's permeability k [m/s], stiffness E [kPa] and the unit weight of the pore fluid γ_w [kPa]. We solve Gibson's theory for sedimentation rate/permeability pairs that result in an overpressure ratio u^*=0.7 in a generic, very soft marine clay. u^* [] is the excess pore water pressure at the base of the sediment column normalised to effective stress due to overburden

(submerged weight of the overlying sediment). γ_w is 10.24 kN/m³ and a stiffness E of 480 kPa is assumed, which represents the lower limit for very soft clay suggested by USACE EM 1110-1-1904.

2.2 Finite Element Modelling of Two-Dimensional Slopes

A 2D plane strain nonlinear elastoplastic coupled pore pressure-deformation model was developed using the finite element (FE) software package ABAQUS. We use the Modified Cam Clay model (Roscoe and Burland 1968) with isotropic nonlinear elasticity and constant Poisson ratio ν. The slope of the critical state line M [] is a constant and is calculated from the friction angle φ_{crit}' [°] by

$$M = \frac{\sin\varphi_{crit}' \cdot 6 \cdot \sqrt{1-b+b^2}}{3+\sin\varphi_{crit}' \cdot 2b - \sin\varphi_{crit}'} \quad (1)$$

where b=0.5 for plane strain conditions (Potts and Zdravkovicz 2001). Strain hardening is exponential. Void ratio changes due to effective stress changes are controlled by the logarithmic bulk modulus (or compression index) λ []. The sediment is cohesionless and its coefficient of earth pressure K_0 [] equals $1-\sin\varphi_{crit}'$. Table 1 lists the constants that define the constitutive model consistent with a calcareous marine clay as typically found off NW Africa.

A simplified continental margin geometry is adopted based on the morphology of the NW African margin and is shown in Figure 2. The entire continental margin is modelled as one layer without abrupt material changes and only vertical (not lateral) density and permeability gradients. The model domain is partitioned into region 1, which comprises the upper 500 m of the seafloor and region 2, which covers the deeper part. The mesh consists of 76,050 rectangular plane strain elements and 238,347 nodes. Elements have a size of 10x10 m at the seafloor, whilst a coarser mesh size (100x100 m) was adopted at 500 m below the seafloor as changes in mechanical properties are less pronounced at these deeper levels (Hamilton 1976, Karig and Hou 1990). Element sizes further increase towards the model's bottom as well as towards lateral boundaries at both sides.

Boundary conditions are given in Figure 2. Sedimentation is simulated by progressively adding a vertical surface load that decreases from the shelf edge towards the abyssal plain. At the shelf the rate is uniform. The exponential rate of decrease ($e^{-0.032x}$, where x [km] is the distance from the shelf edge) is based upon thinning rates of seismic sequences in Antobreh and Krastel (2007). A unit weight, γ=12 kN/m³, was assumed for the newly deposited fully saturated sediment corresponding to a dry density of 670 kg/m^3. The peak sedimentation rate at the shelf edge is 0.15 m/ka.

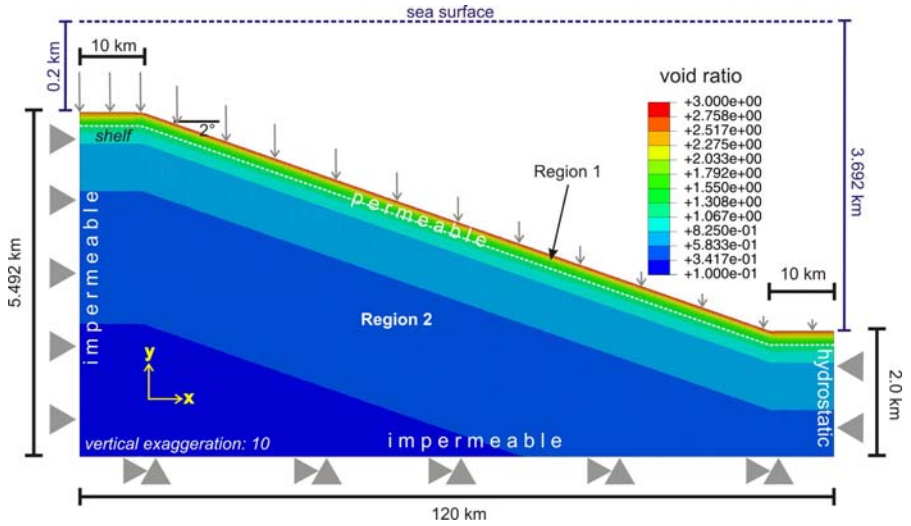

Fig. 2. 2D slope model geometry (not to scale) with boundary and loading conditions. Pore pressure at the right boundary is hydrostatic so that flow into or out of the model is allowed. As deposited sediment is simulated as a surface load at the seafloor, the flow normal to the surface is governed by the pore pressure gradient and the vertical permeability. The seafloor is free to move in any direction whereas the side boundaries are fixed in the x direction and the bottom is fixed in both directions. The water column is represented as a hydrostatic pressure load on the seafloor, such that there is zero effective stress at the seafloor. Sedimentation decreases exponentially from the shelf edge towards the abyssal plain (grey vertical arrows). Colours represent the initial void ratio on which permeability and density depend linearly.

2.2.1 Initial conditions

Seafloor sediments are considered normally consolidated and have an initial void ratio of 3.0 (75% volume porosity). Sediment porosity φ and void ratio *e* are related by $\varphi = e/(1+e)$. In the interval 0 to 500 m below the seafloor (region 1) φ is defined by

$$\varphi = 0.75 \cdot 0.987z + 0.83z^2 \qquad (2)$$

where *z* [km] is the depth below the seafloor after Hamilton (1976) for calcareous sediments. In region 2 porosity decreases linearly from 40% at 500 m below the seafloor, to 10% at 5000 m below the seafloor (Velde 1996).
Permeability depends linearly on void ratio and is anisotropic, as measured for pelagic clay (Kawamura and Ogawa 2004). The horizontal sediment permeability k_x at the seafloor before burial (where e=3.0), is 10^{-8} m/s based on oedometer measurements of calcareous sediments compiled by Demars (1982). Yang and

Aplin (2010) found vertical permeability k_y as low as 10^{-13} m/s for mudstones with 40% porosity, which we use as the lower limit for vertical permeability variations. Below 500 m (region 2) k is isotropic and constant (k=10^{-13} m/s). In our models we keep the permeability at the seafloor constant and varied k at 500 m as well as the anisotropy coefficient in order to explore model sensitivity. k_y can be up to one order of magnitude smaller than k_x.
Sediment at the seafloor has a dry density of 670 kg/m³ (γ=12 kN/m^3) that increases linearly to 1400 kg/m³ at 500 m depth (γ=20 kN/m³). Sediment more than 500 m below the seafloor has constant density of 2400 kg/m³ (γ=26 kN/m³).

Notation		Value	Reference
κ	Swelling index	0.027	Valent et al. (1982), Demars (1982)
ν	Poisson ratio	0.3	Karig and Hou (1993)
λ	Compression index	0.28	Valent et al. (1982), Demars (1982)
φ_{crit}' [°]	Friction angle	28	Valent et al. (1982)
M	Slope of critical state line	0.87	Equation (1), b=0.5
γ_w [kN/m³]	Specific weight of fluid	10.24	
g [m/s²]	Gravity	9.81	

Table 1. Spatially and temporarily constant input parameters used in the Modified Cam Clay constitutive model.

2.2.2 Key Assumptions

The continental margin is simulated as one layer (no abrupt property changes) to investigate whether failure could occur without the need for weak layers or glide planes. This effectively assumes spatially uniform deposition of the same material in space and time. Geotechnical properties have not been measured on deep sediments off NW Africa. Those properties used in this model are thus based on a literature review for calcareous pelagic and hemipelagic sediments measured elsewhere (Hamilton 1976, Velde 1996, Yang and Aplin 2010, and references in Table 1). The FE model is comparatively simple; it does not include geometric nonlinearity and the deposited sediment is simulated by a surface load. The latter is important because it means that the added sediment is not a source of fluid, and possible failure within the additional sediment thickness cannot be modelled. However, this model serves to explore the general relationships between sediment accumulation rates and permeability in a continental slope with a geometry broadly similar to that of the NW African margin, Gulf of Mexico or Norwegian margin.

3. Results

3.1 One-Dimensional Consolidation

High sedimentation rates for prolonged periods of time, and low permeability and stiffness, tend to result in high overpressure. Our 1D modelling indicates that a significant overpressure ratio of u^*=0.7 does indeed build up in settings with rapid sediment accumulation, such as the Gulf of Mexico (after sedimentation periods of about 50 ka) and the Norwegian continental slope after 10 ka (Fig. 3; Leynaud et al. 2007, Flemings et al. 2008). When sedimentation is ~500 times slower (0.15 m/ka) as in the case of the NW African margin, the permeability must be lower than 10^{-12} m/s and continuous sedimentation must go on for long periods (>1.5 Ma) to generate significant overpressure ratio. Such low values of permeability have been measured perpendicular to bedding for mudstones with clay content >50% and porosities <30% (Yang and Aplin 2010). However, the average clay content of sediment at the NW African margin is about 25% and the porosity at 300 m depth below seafloor is 50% (Ruddiman et al. 1988). The occurrence of permeabilities $<10^{-12}$ m/s in a sediment as found off NW Africa is thus unlikely, but cannot be fully excluded as clay mineral accumulation may peak locally. Due to sparse data coverage, especially at greater depths, this is not well constrained and requires further investigation. With a higher but more realistic permeability of 10^{-9} m/s (Demars 1982), the overpressure ratio is negligible and the slope is not close to failure.

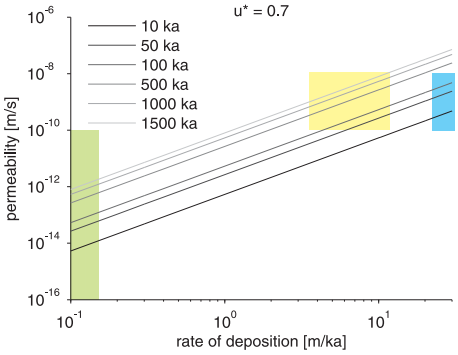

Fig. 3. Log-log plot of combinations of permeability and sedimentation rate that result in an overpressure ratio $u^* = 0.7$ at the base of a consolidating layer for time periods of 10 ka to 1.5 Ma after Gibson (1958). All parameters are assumed constant. The bottom boundary is impermeable. Shaded backgrounds highlight typical sedimentation rate ranges off NW Africa (green) as well as sedimentation rate and permeability ranges in the Gulf of Mexico (yellow) and off Norway (blue). A stiffness of 480 kPa is used for all calculations.

3.2 Two-Dimensional Consolidation

Several numerical experiments with different vertical permeability gradients and anisotropy ratios were run for 1 Ma. Slope stability is evaluated by analysing

vertical effective stresses, σ_v', overpressure ratios, u^*, and Factors of Safety (FoS, ratio of the critical state friction angle to the mobilised friction angle). In summary, all models are stable. All simulations show an expected increase in vertical effective stress and pore pressure due to the overburden. Fluid flow patterns vary within the different models and lateral flow is observed in the models with permeability anisotropy but does not generate significant overpressure ratios at the lower slope. Where permeability is isotropic, fluid flow is purely vertical.

To give an example, Figure 4 shows the model with lowest permeability (k_x decreasing from 10^{-8} to 10^{-12} m/s at 500 m depth, k_x/k_y=10) and a sedimentation rate of 0.15 m/ka at the shelf. The σ_v' contour lines are not parallel to the slope; with higher values at the shelf and lower values towards the foot of the slope (Fig. 4a). This is due to asymmetric loading. σ_v' does not show any abnormal pattern and is nowhere near zero.

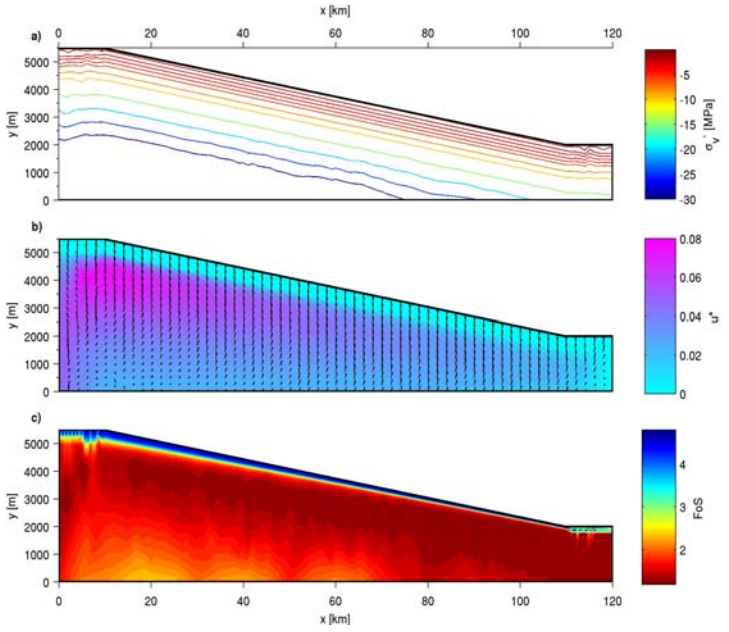

Fig. 4. 2D FE solution for vertical effective stress σ_v' (a), overpressure ratio u^* with flow velocity vectors normalised to their absolute magnitude (b), and Factor of Safety calculated at each node (c) after continuous loading with 0.15 m/ka for 1 Ma. Vertical exaggeration is 5.

The maximum overpressure ratio u^* is 0.074 near the shelf edge and at a sub-seafloor depth of about 1500 m (Fig. 4b). However, in the top 500 m u^* is significantly lower. Fluid flow has a small component towards the foot of slope but is predominantly vertical (as shown by black vectors in Fig. 4b).

The FoS is as low as 1.3 below the shelf edge, and from x >60 km (Fig. 4c) at sub-sea floor depths of about 2000 m and greater than 300 m, respectively. Undulations of the contour lines near both side boundaries are due to coarse meshing in that area. The FoS contour lines along the slope converge towards the lower slope indicating that the lower slope is less stable than the upper slope, especially at shallow depths. Nevertheless, FoS is >1 everywhere in the model and so no failure mechanism could be identified.

4. Discussion

Previous 1D and 2D slope modelling suggests that rapid (peaking at ~30 m/ka) and prolonged (several ka) sediment deposition from river discharges or ice streams can generate sufficiently high over-consolidation ratios (u^*>0.7) to make a continental slope unstable (Leynaud et al. 2007, Flemings et al. 2008). However, our modelling suggests that such large pressurisation ratios are not generated in locations such as the NW African margin where sedimentation rates are much lower (0.01 to 0.15 m/ka), for reasonable values of initial permeability and changes of permeability with depth.

Our work therefore suggests that large-scale failures of slope made of homogeneous low-permeability sediment are in at least some cases not generated by rapid sediment loading alone (perhaps with lateral fluid flow to the toe of slope). It appears that layers of anomalously low permeability that prevent fluid migration, or high permeability layers that allow more rapid lateral fluid flow would be needed. Alternatively, weak layers must be present, all of which are not included in our modelling.

If weak layers are needed for low angle slope failure in areas of slow sedimentation, what are those weak layers? It has been suggested that dissociation of gas hydrates could produce weak layers in a number of ways including rapid removal of cement to leave sediment under-consolidated, formation of voids (gas bubbles) and fractures, and freshening of pore fluids leading to quick clay behaviour (e.g. Bull et al. 2009). All three margins considered here show evidence for gas hydrate occurrence (Sager et al. 1999, Bouriak et al. 2000, Davies et al. 2010). However, slide headscars in the Gulf of Mexico and off NW Africa are located at water depths well below the gas hydrate stability zone (Wynn et al. 2000, Twichell 2009). Shifts of the upper end of the gas hydrate stability zone therefore are unlikely to affect sediments near the headscars. We therefore conclude that gas hydrates as a trigger can be excluded. It appears that some other mechanism is capable of producing weak layers in locations offshore NW Africa, and potentially also in other locations where sedimentation rates are greater.

References

Antobreh AA, Krastel S (2007) Mauritania slide complex: morphology, seismic characterisation and process of formation. Int J Earth Sci 96: 451-472.

Bouriak S, Vanneste M, Saoutkine A (2000) Inferred gas hydrates and clay diapirs near the Storegga slide on the southern edge of the Voring plateau, offshore Norway. Mar Geol 163: 125-148.

Bull S, Cartwright J, Huuse M (2009) A subsurface evacuation model for submarine slope failure. Basin Research 21: 433-443.

Davies RJ, Clarke AL (2010) Methane recycling between hydrate and critically pressured stratigraphic traps, offshore Mauritania. Geol 38: 963- 966.

Demars KR (1982) Unique engineering properties and compression behavior of deep-sea calcareous sediments. In: Demars KR, Chaney RC (eds) Geotechnical properties, behavior and performance of calcareous soils, ASTM, Philadelphia.

Flemings PB, Long H, Dugan B, Germaine JT, John CM, Behrmann JH, Sawyer DE, et al. (2008) Erratum to "pore pressure penetrometers document high overpressure near the seafloor where multiple sub- marine landslides have occurred on the continental slope, offshore Louisiana, Gulf of Mexico". Earth Planet Sci Lett 274: 269-283.
Gibson RE (1958) The progress of consolidation in a clay layer increasing in thickness with time. Geotech 8 (2): 171-182.
Haflidason H, Lien R, Sejrup HP, Forsberg CF, Bryn P (2005) The dating and morphometry of the Storegga slide. Mar Pet Geol 22: 123-136.
Hamilton EL (1976) Variations of density and porosity with depth in deep-sea sediments. J Sediment Pet 46 (2): 280-300.
Henrich R, Hanebuth TJJ, Krastel S, Neubert N, Wynn RB (2008) Architecture and sediment dynamics of the Mauritania slide complex. Mar Pet Geol 25 (1): 17-33.
Karig DE, Hou G (1992) High-stress consolidation experiments and their geological implications. J Geophys Res 97 (B1): 289-300.
Kawamura K, Ogawa Y (2004) Progressive change of pelagic clay microstructure during burial process: examples from piston cores and ODP cores. Mar Geol 207: 131-144.
Krastel S, Wynn RB, Geersen J, Henrich R, Georgiopoulou A, Meyer M, Schwenk T (this volume) Large scale mass wasting at the NW-African Continental Margin: some general implications for mass wasting at passive continental margins.
Leynaud D, Sultan N, Mienert J (2007) The role of sedimentation rate and permeability in the slope stability of the formerly glaciated Norwegian continental margin: the Storegga slide model. Landslides 4: 297-309.
Potts DM, Zdravkovic L (2001) Finite Element analysis in geotechnical engineering. Theory. Thomas Telford.
Roscoe KH, Burland JB (1968) On the generalised stress-strain behaviour of 'wet' clay. In: Engineering plasticity. Cambridge University Press: pp. 535-609.
Ruddiman WF, Sarnthein M et al. (1988) Proc ODP 108, ODP Initial Reports.
Sager WW, Lee CS, Macdonald IR, Schroeder WW (1999) High- frequency near-bottom acoustic reflection signatures of hydrocarbon seeps on the northern Gulf of Mexico continental slope. Geo-Mar Lett 18: 267- 276.
Sarnthein M, Thiede J, Pflaumann U, Erlenkeuser U, Fütterer D (1982) Atmospheric and oceanic circulation patterns off Northwest Africa during the past 25 million years. In: von Rad U (ed) Geology of the Northwest African continental margin. Springer Verlag, Berlin: 545-604.
Stigall J, Dugan B. (2010) Overpressure and earthquake initiated slope failure in the Ursa region, northern Gulf of Mexico. J Geophys Res 115 (B04101).
Twichell DC, Chaytor JD, ten Brink US, Buczkowski B (2009) Morphology of late quaternary submarine landslides along the U.S. Atlantic continental margin. Marine Geology 264: 4-15.
Valent PJ, Altschaeffl AG, Lee HJ (1982) Geotechnical properties of two calcareous oozes. In: Demars KR, Chaney RC (eds) Geotechnical properties, behavior and performance of calcareous soils, ASTM, Philadelphia.
Velde B (1996) Compaction trends of clay-rich deep sea sediments. Mar Geol 133: 193-201.
Wynn RB, Masson DG, Stow DAV, Weaver PPE (2000) The northwest African slope apron: a modern analogue for deep-water systems with complex seafloor topography. Mar Pet Geol 17: 253- 265.
Yang Y, Aplin AC (2010) A permeability-porosity relationship for mudstones. Mar Pet Geol 27: 1692-1697.

Acknowledgments

Sebastian Krastel kindly provided reflection seismic lines offshore NW Africa. Brandon Dugan, Peter Flemings and Derek Sawyer are thanked for their encouragement to address these problems. We also thank the reviewers C. Berndt and A. Kopf for their constructive reviews.